

Physical forcing and phytoplankton distributions

TREVOR PLATT¹, HEATHER BOUMAN², EMMANUEL DEVRED²,
CÉSAR FUENTES-YACO^{2,1} and SHUBHA SATHYENDRANATH²

¹ Bedford Institute of Oceanography, Box 1006, Dartmouth, Nova Scotia, Canada B2Y 4A2. E-mail: tplatt@dal.ca

² Oceanography Department, Dalhousie University, Halifax, Nova Scotia, Canada B3H 4J1.

SUMMARY: At the global and regional scales, the distribution and abundance of marine phytoplankton are under the control of physical forcing. Moreover, the community structure and the size structure of phytoplankton assemblages also appear to be under physical control. Areas of the ocean with common physical forcing (ecological provinces) may be expected to have phytoplankton communities that respond in a similar fashion to changes in local forcing, and with ecophysiological rate parameters that are predictable from local environmental conditions. In modelling the marine ecosystem, relevant parameters may be assigned according to a partition into ecological provinces. To the extent that physical forcing of the ocean is not constant within or between years, the boundaries of the provinces should be considered as dynamic. The dynamics and the associated changes in taxa can be revealed by remote sensing.

Keywords: phytoplankton, pigments, remote sensing, ocean colour, diatoms, hurricane, biogeochemical provinces.

RESUMEN: INFLUENCIA DE FACTORES FÍSICOS Y DISTRIBUCIÓN DE FITOPLANCTON. – A escalas global y regional, la distribución y abundancia del fitoplancton marino están controladas por factores físicos. Además, la composición y la estructura de tamaños de las comunidades fitoplanctónicas también parecen estar gobernadas por factores físicos. En áreas del océano sujetas al mismo tipo de influencias físicas (provincias ecológicas) cabría esperar que las comunidades fitoplanctónicas respondieran de forma similar a cambios locales y presentaran tasas de parámetros ecofisiológicos predecibles a partir de las condiciones ambientales locales. Por ello, parámetros relevantes para la modelización de ecosistemas marinos pueden asignarse en base a una partición del océano en provincias ecológicas. Teniendo en cuenta que los factores físicos que influyen en los océanos no son constantes ni intra ni interanualmente, los límites de estas provincias deberían ser considerados como variables. La dinámica de esta variabilidad y los cambios de composición taxonómica asociados a ella pueden ser observados mediante sensores remotos.

Palabras clave: fitoplancton, pigmentos, sensores remotos, color del océano, diatomeas, huracan, provincias biogeoquímicas.

INTRODUCTION

In the natural environment the photosynthetic response of phytoplankton to available light is not constant, but varies according to the physiology of the cells, which is governed by their size, taxonomic composition and the environmental conditions (temperature, nutrients, light) in which they live. For various applications, such as the computation of primary production at large geographic scales (Platt and Sathyendranath, 1999), we often need to quantify this response for places and times at which we

have no observational data. Quantifying the response is equivalent to assigning magnitudes to the parameters of the relationship between photosynthesis and available light. This means that we must extrapolate the (usually) limited observational data to cover all the times and places of interest. One approach to the problem of extrapolating the photosynthesis parameters of marine phytoplankton over large spatial scales (Platt and Sathyendranath, 1988) is to partition the ocean into provinces, each having seasonally-predictable algal growth dynamics. The criteria for the assignment of provinces are

based on our knowledge of biological responses in the phytoplankton to oceanographic forcing.

In a practical implementation, the boundaries of the provinces may be drawn as if fixed in time and space. However, it is understood that in reality, the boundaries are free to vary (Platt and Sathyendranath, 1999) in response to variations in the physical forcing on which they are based. If the assignment of provincial boundaries is to be dynamic, it should be based on remotely-sensed observables, such as sea-surface chlorophyll and temperature fields, so that the boundaries can be treated with high spatial resolution and updated according to the available repeat coverage. Assigning each pixel in the remotely-sensed image to a particular province based on that image and on other remotely-sensed data would be the first step in the computation of primary production at large scales in the operational mode.

It has been shown that phytoplankton size structure and taxonomic composition vary with changes in physical forcing and nutrient availability. In general, large cells tend to dominate where nitrate concentrations are high, whereas smaller cells are characteristic of highly-stratified waters in which regenerated forms of nitrogen are found (Margalef, 1978; Yentsch and Phinney, 1989; Chisholm, 1992; Cullen *et al.*, 2002). Although the evidence for a link between physical forcing and phytoplankton size structure is largely qualitative, a few quantitative studies also support this view. Using an empirical model, Rodríguez *et al.* (2001) demonstrated that the relative abundance of large cells increases with the magnitude of mesoscale vertical motion. Li (2002) reported a strong relationship with size structure of phytoplankton and the degree of water-column stability. Of course, it is difficult to separate the relative influences that turbulence and nutrient availability have on phytoplankton community structure, since hydrodynamic forcing is also the principal mechanism responsible for the transport of nutrients from the deep ocean to the photic zone.

Temperature is one of the most frequently-measured environmental variables in the ocean and it can be observed routinely over large scales by satellite. Although temperature itself is an important factor governing the distribution of phytoplankton in the ocean, it also provides a quantitative index of the physico-chemical state of the marine environment. For example, we know that the seasonal warming of surface waters in the temperate open ocean is the primary mechanism responsible for strengthening

the stability of the water column, which causes a reduction in the flux of nutrients from below the mixed layer during the summer months. Thus, increasing sea-surface temperatures are associated with a strengthening in the density gradient, and a corresponding decrease in the diffusion of nutrients across the pycnocline. This link between sea-surface temperature and nitrate concentration has been exploited in studies that attempt to estimate the concentration of nitrate over regional (Sathyendranath *et al.*, 1991) to global scales (Carder *et al.*, 1999; Switzer *et al.*, 2003), using temperature fields obtained by satellites.

The importance of temperature as a predictor of many of the patterns and processes in phytoplankton ecology has been shown repeatedly in the literature. Using measurements of pigment composition, cell size and phytoplankton absorption, Bouman *et al.* (2003) showed that the size and gross taxonomic structure of phytoplankton follow changes in temperature for a variety of oceanic regions. Li (in press) has shown that the abundance of the ubiquitous picoplankter *Synechococcus* is strongly correlated with temperature for samples collected in the North-West Atlantic.

The rate of light-saturated photosynthesis (the assimilation number) has also been shown to be temperature dependent in temperate marine ecosystems. Although this relationship has usually been attributed in the past to the enzymatic nature of the dark reactions of photosynthesis (Geider and Osborne, 1992), some workers have also suggested that the relationship may be a result of the concomitant change in phytoplankton size and taxonomic structure with temperature (Platt and Jassby, 1976; Côté and Platt, 1983; Bouman *et al.*, in press). Using a pelagic food web model, Laws *et al.* (2000) found that temperature explained a significant proportion of the variance in measurements of the ratio of export to total production taken from the literature. Thus, the potential use of temperature to provide information on the structure and function of the pelagic ecosystem is well established.

Chlorophyll is the pigment involved in the conversion of inorganic carbon to organic compounds usable as a substrate to sustain the aquatic ecosystem. Because it is unique to photosynthetic organisms, it provides a useful marker of the biomass of the autotrophic community. Its function to absorb light for photosynthesis gives it an optical signature that can be detected from space. In addition to its primary role as an indicator of phytoplankton bio-

mass, chlorophyll concentration has also been proposed as a proxy index of phytoplankton size structure. A conventional view is that there exists a constant background of picoplanktonic cells and that, as nutrient availability increases, there is a corresponding increase in the abundance of larger cells (Yentsch and Phinney, 1989; Chisholm, 1992). Data collected in the North-West Atlantic, however show that the pico-phytoplankton actually decrease as pigment concentration increases and that the nano-phytoplankton show limited variability with chlorophyll concentration (Li, 2002). Nevertheless, the hypothesis that the relative proportion of micro-phytoplankton increases as chlorophyll concentration increases, still holds (Rodríguez *et al.*, 1998).

Although the main product of ocean-colour data is chlorophyll concentration, recent studies have shown that information on the size structure and taxonomic composition of marine phytoplankton may be derived from the remotely-sensed signal (Ciotti *et al.*, 1999, 2002), using relationships between chlorophyll and cell size of the type outlined above. Sathyendranath *et al.* (2004) established an algorithm to detect the presence of diatoms using satellite data of ocean colour. Thus, if robust relationships could be established between phytoplankton functional groups and photosynthetic performance, then information on their relative contribution to the autotrophic community might be used as an aid to the assignment of photosynthesis-irradiance parameters over basin scales.

Here, we attempt to establish an ecological geography of the North-West Atlantic Ocean using two ocean observables: sea-surface temperature and chlorophyll concentration. We begin by examining the correlations of both temperature and chlorophyll-*a* concentration with two indices of phytoplankton community structure (pigment composition and phytoplankton absorption characteristics) and with photosynthetic parameters. We then propose a method for assigning dynamic boundaries to the biogeochemical provinces of the North-West Atlantic using remotely-sensed data on sea-surface temperature and chlorophyll. These boundaries are compared with the distribution of diatom populations as determined by remote-sensing, to assess whether the boundaries are consistent with the known ecological diversity of the study region. Next, using hurricanes off the Grand Banks in a case study, we demonstrate how this dynamic approach is able to embrace ecologically-important episodic events in physical forcing.

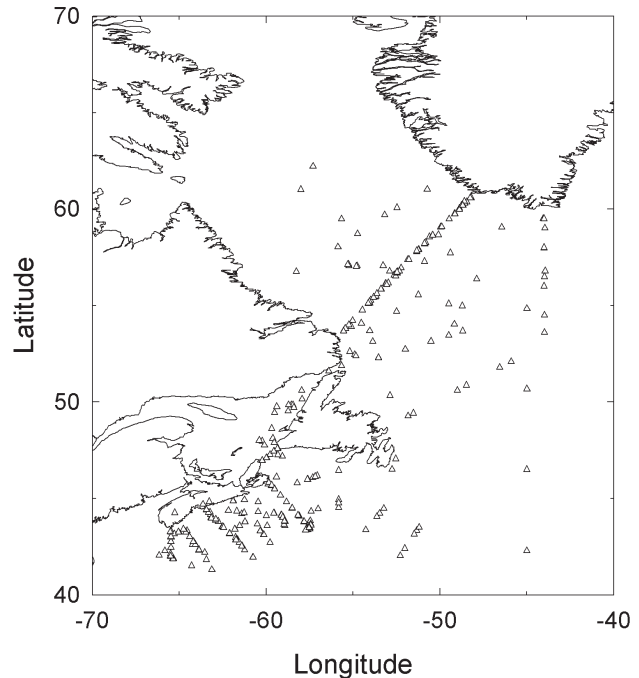


FIG. 1. – Map showing stations sampled during 15 cruises of the Scotian Shelf and Labrador Sea.

REMOTELY-SENSED OBSERVABLES AND PHYTOPLANKTON STRUCTURE AND FUNCTION

To examine the predictability of phytoplankton composition and photosynthetic performance from remotely-detectable variables, we used data collected on 15 cruises to the Scotian Shelf and Labrador Sea during the period of May 1996 to December 2003 (Fig. 1). Measurements of temperature were obtained from a SeaBird CTD profiler. Pigment composition was obtained using High Performance Liquid Chromatography (HPLC) according to the method of Head and Horne (1993).

Two indices of phytoplankton community structure were used in this study. The first is the pigment index F_μ , which represents the contribution of micro-phytoplankton cells to the total pigment biomass (Claustre, 1994) based on the relative concentration of accessory pigments obtained by HPLC. The index is simply the sum of diagnostic pigments associated with large cells (diatoms and dinoflagellates) divided by the sum of diagnostic pigments associated with all phytoplankton size classes:

$$F_\mu = \frac{D_f + D_p}{D_f + D_p + D_h + D_b + D_a + D_c + D_z} \quad (1)$$

where D_f and D_p represent the concentrations of the carotenoids fucoxanthin and peridinin, respectively.

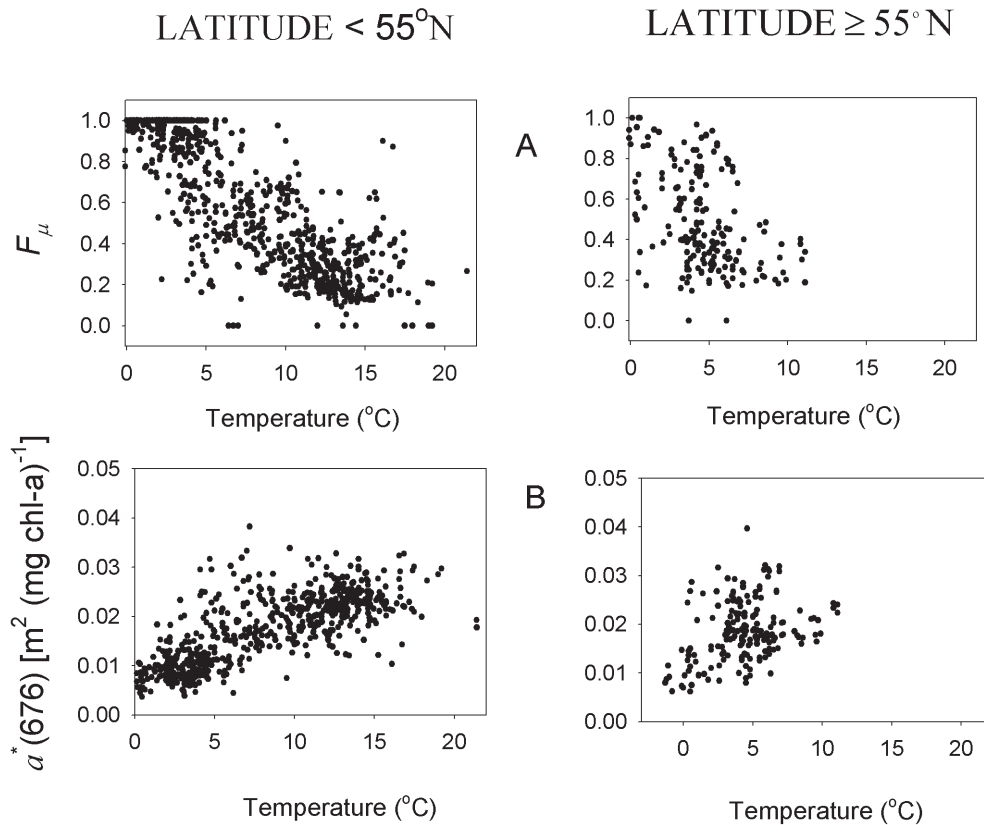


FIG. 2. – Plot of two indices of community structure against temperature for low-latitude and high-latitude regions. A) The pigment index F_{μ} (Equation 1) and B) the chlorophyll-a specific absorption coefficient at 676 nm, $a^*(676)$.

The concentrations of 19' hexanoyloxyfucoxanthin, 19' butanoyloxyfucoxanthin and alloxanthin are represented by D_h , D_b and D_a respectively. These are three carotenoids associated with the nano-phytoplankton size class. Chlorophyll-b (D_c) and zeaxanthin (D_z) are pigments associated with the pico-phytoplankton size class.

The second index of phytoplankton community structure is the chlorophyll-a specific absorption coefficient at 676 nm, $a^*(676)$ (Bouman *et al.*, 2003). Phytoplankton absorption coefficients were obtained using the filter pad method. Briefly, algal cells were filtered onto a glass fibre filter, and the filter was scanned from 350 to 750 nm using a Shimadzu dual-beam spectrophotometer with an integrating sphere assembly. Pigments were extracted from the GF/F filter as described in Bouman *et al.* (2003) and the filter was re-scanned to obtain the optical density of detrital material. Optical density was converted to absorption coefficient (Hoepffner and Sathyendranath, 1992, 1993), and the difference between total particulate absorption and the absorption by detrital material yielded the absorption by phytoplankton. The absorption

coefficient of phytoplankton at each wavelength was divided by the concentration of chlorophyll-a in the sample, to obtain the specific absorption coefficient ($\text{m}^2 \text{mg Chl-a}^{-1}$). The specific absorption coefficient at the red absorption peak of chlorophyll-a (676 nm) is little affected by changes in pigment composition, but is affected by the size of the cells, through the flattening effect (Duysens, 1956). Hence, the specific absorption coefficient at 676 nm is used here as an index of phytoplankton cell size, as in Bouman *et al.* (2003).

Photosynthesis-irradiance experiments were conducted at sea. Water samples were inoculated with ^{14}C radioisotope and incubated in an artificial light gradient for three hours. Photosynthesis-irradiance curves derived from the experiments were fitted to the equation of Platt *et al.* (1980) to obtain the photosynthesis-irradiance parameters, P_m^B , the photosynthetic rate at saturation (also known as assimilation number) and α^B , the initial slope of the curve.

The results from samples collected only in the top 20 m of the water column are shown in this study, for two reasons. First, the remotely-sensed signals of both temperature and ocean colour are

heavily weighted towards the sea surface. Second, by focussing on data collected near the sea surface, variability in the optical and photosynthetic characteristics of phytoplankton caused by photoacclimation of cells to low light levels at depth is minimised.

For samples collected south of 55°N a clear temperature-dependence for both indices of phytoplankton community structure is observed (Fig. 2). A possible explanation for this relationship lies in the link between vertical density structure and temperature. At higher latitudes, however, neither phytoplankton pigment composition nor specific absorption appear to be related to temperature. This lack of correlation between temperature and phytoplankton community structure in higher latitudes may be, in part, a result of a significant contribution of salinity, rather than temperature, to the vertical density structure.

Chlorophyll and our indices of community structure show similar relationships for both latitudinal ranges (Fig. 3). At chlorophyll-a concentrations <5 mg m⁻³, values of both F_{μ} and $a^*(676)$ are highly variable, covering the entire range possible (0 to 1 for F_{μ} , and 0.003 to 0.06 m² (mg Chl-a)⁻¹ for $a^*(676)$). Thus at low-to-intermediate concentrations of chlorophyll, cells covering a wide range of sizes

and taxonomic groups may be present. At chlorophyll-a concentrations > 5 mg Chl-a m⁻³, however, values of F_{μ} and $a^*(676)$ imply the dominance of large cells (diatoms) exclusively, with high relative concentrations of the indicator pigment fucoxanthin and low specific absorption coefficients. Thus it would appear that in bloom conditions in this region, where chlorophyll concentrations reach values greater than 5 mg Chl-a m⁻³, the phytoplankton are often dominated by diatoms, though *Phaeocystis* blooms are also known to occur.

Since community structure appears to vary in a regular way with temperature, and since both phytoplankton taxonomic composition and temperature are known to be sources of variability in the photosynthetic parameters in the natural environment, we would anticipate that temperature would be a good indicator of the photosynthetic properties of marine phytoplankton in this region. When the light-saturated photosynthetic rate, represented by the parameter, P_m^B , is plotted against temperature, a strong temperature-dependence is revealed (Fig. 4). This is in agreement with numerous studies conducted in temperate waters that also show a positive correlation between temperature and light-saturated photosynthesis. Many studies have attributed the correla-

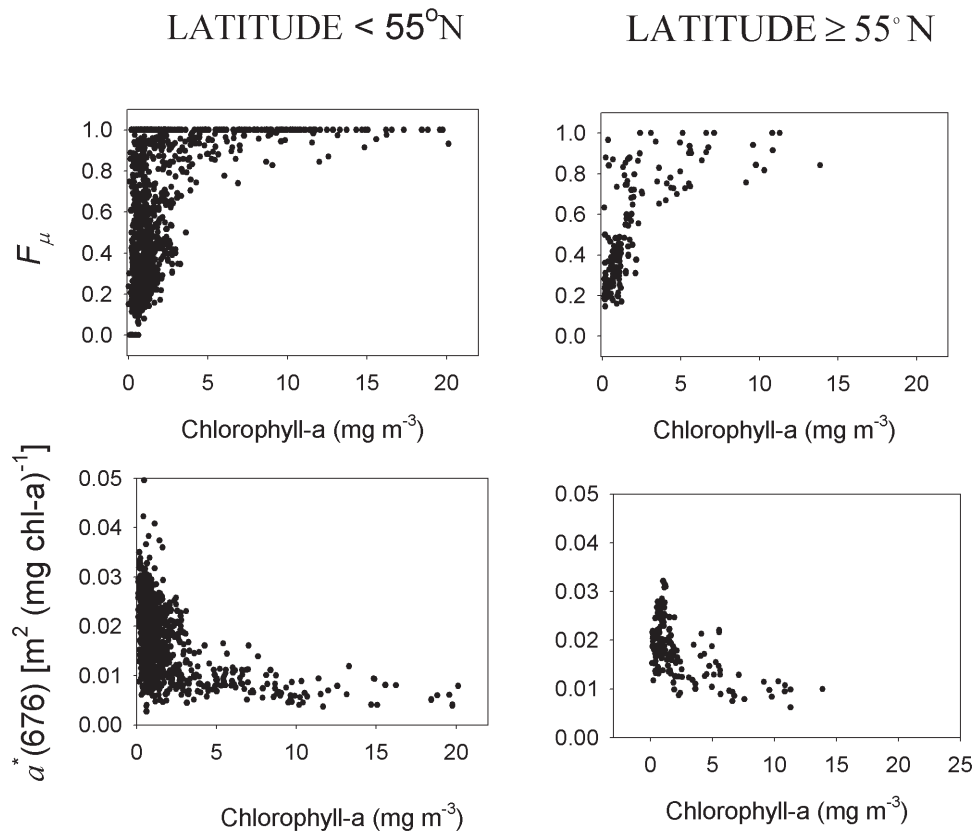


FIG. 3. – Plot of two indices of community structure against chlorophyll-a concentration for low-latitude and high-latitude regions.

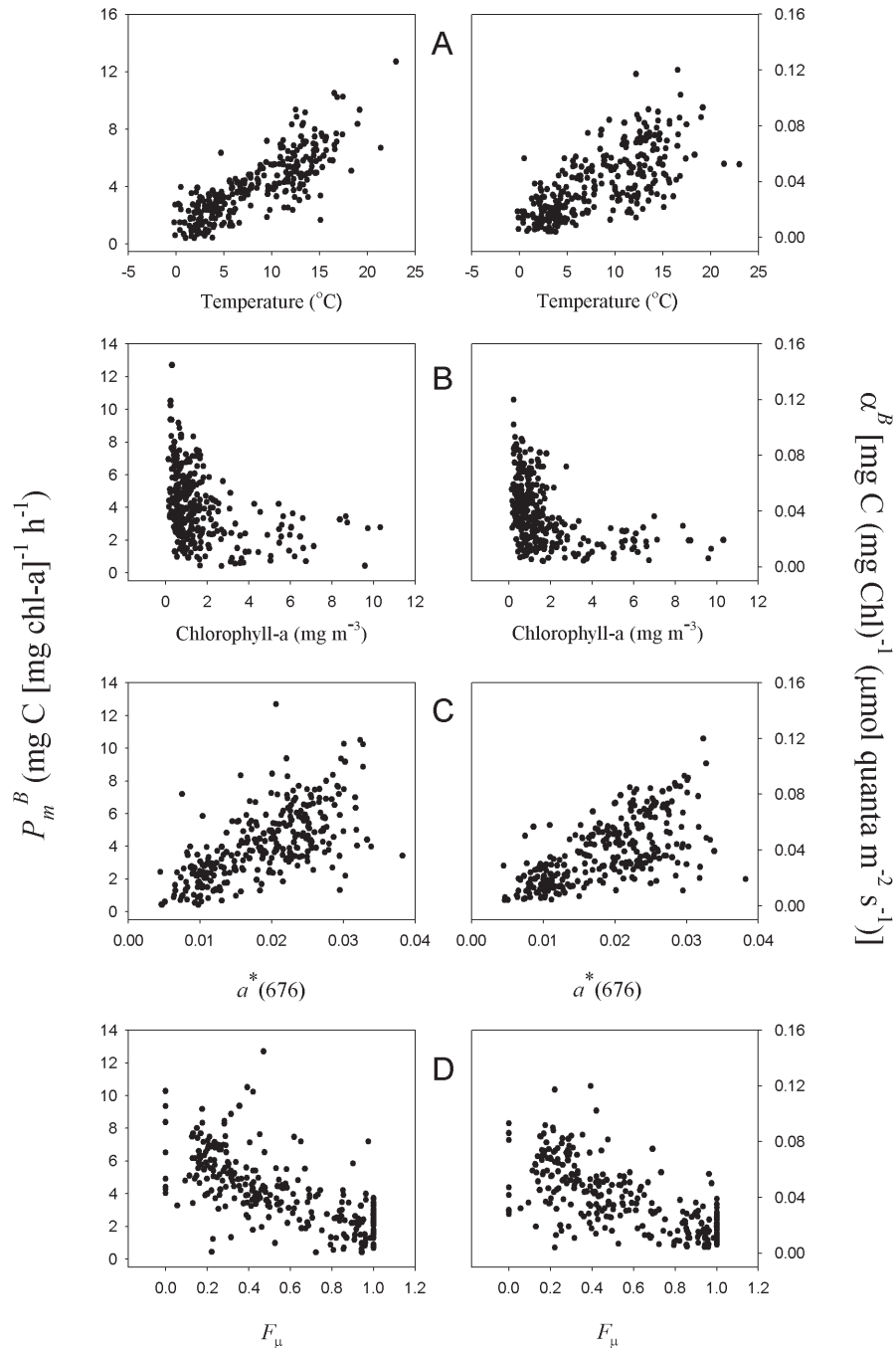


Fig. 4. – Plot of the photosynthetic parameters against A) temperature, B) chlorophyll-a concentration C) the chlorophyll-specific absorption coefficient at 676 nm, $a^*(676)$ and D) the pigment index F_{μ} (Equation 1).

tion between P_m^B and temperature to a direct effect of temperature impacting the enzyme-controlled dark reactions of photosynthesis (Geider and Osborne, 1992). It should be pointed out, however, that the temperature-dependence of light-saturated photosynthesis has been shown to be weak or absent in other oceanic regimes (Behrenfeld *et al.*, 2002, Bouman *et al.*, in press). This lack of dependence has been attributed to several factors, including vari-

ability in the concentration of the enzymes involved in the Calvin cycle and in the intracellular chlorophyll concentration with changes in ambient temperature (Behrenfeld *et al.*, 2002). In addition, changes in nutrient stress (Eppley *et al.*, 1972) and phytoplankton community structure (Bouman *et al.*, in press) have also been implicated.

When the initial slope of the photosynthesis-irradiance curve, α^B , is plotted against temperature, a clear

positive relationship is also found (Fig. 4A). It is difficult to invoke a direct causative factor to explain this relationship: unlike the case for P_m^B , no physiological basis has been invoked to explain this apparent dependence of α^B on temperature. Thus we must conclude that there is another co-variate or a group of covariates governing the relationship. To examine the influence of phytoplankton community structure on the photosynthetic parameters, P_m^B and α^B are plotted against $a^*(676)$ and F_μ (Fig. 4C and D). Both the photosynthetic parameters P_m^B and α^B appear to be strongly correlated with $a^*(676)$. The relationship between the initial slope of the photosynthesis-irradiance curve (α^B) and $a^*(676)$ is not surprising, since α^B is related to the absorptive efficiency of phytoplankton according to the following relationship:

$$\alpha^B = \phi_m \bar{a}^* \quad (2)$$

where \bar{a}^* is the spectrally-averaged specific absorption coefficient of phytoplankton and ϕ_m is the realised maximum quantum yield of photosynthesis (Platt and Jassby, 1976; Geider and Osborne, 1992). The relationship between P_m^B and $a^*(676)$ is more difficult to interpret. Yet, if we assume that $a^*(676)$ is an index of phytoplankton cell size, then perhaps this relationship can be rationalised. Geider *et al.* (1986) demonstrated that both \bar{a}^* and the light-saturated maximum growth rate (μ_m) decrease with an increase in cell size. Since under light-saturated conditions, μ_m should be proportional to P_m^B , and since \bar{a}^* is proportional to α^B , both photosynthetic parameters should be size dependent. The positive correlation of $a^*(676)$ with the two photosynthesis parameters implies that smaller cells have higher rates of light-limited and light-saturated photosynthesis per unit biomass than larger cells. The relationship between the pigment index F_μ and the photosynthetic parameters also supports the view that larger cells (diatoms) have lower biomass-specific production rates than smaller cells. These results are consistent with other field (Yentsch and Ryther, 1957; Côté and Platt, 1983, 1984; Bouman *et al.*, in press) and laboratory (Taguchi, 1976; Geider *et al.*, 1986; Finkel, 2001) studies which show that larger cells tend to have lower biomass-specific photosynthetic rates than small cells.

Results obtained in this study point to both temperature and to indices of the size and taxonomic structure of phytoplankton cells as potential indicators of the values of photosynthetic parameters for the North-West Atlantic region. Since temperature

and indices of phytoplankton community structure can be obtained by remote sensing (at least indirectly), they could be used as the basis of a protocol for assignment of photosynthesis parameters to estimate primary production from ocean colour in an operational mode.

Although these relationships appear to be robust for the North-West Atlantic, they may not hold for other oceanic regions. For example, in the Arabian Sea, no relationship between temperature and community structure was apparent in the data collected over a series of cruises during the monsoon and inter-monsoon seasons (Bouman *et al.*, 2003; Bouman *et al.*, in press). However, the relationships of total chlorophyll concentration and pigment indices of taxonomic composition with the photosynthetic parameters were similar to those in the North-West Atlantic. Such regional differences lend additional support to a province-based approach to large-scale computations of primary production.

A DYNAMIC ASSIGNMENT OF ECOLOGICAL PROVINCES USING SATELLITE OBSERVATIONS

As shown in the previous section, sea-surface temperature and chlorophyll biomass can be used in the North-West Atlantic to provide information about phytoplankton functional groups (related to cell size) and their physiological state, and these variables are now measured on a routine basis by several satellite sensors. This opens the avenue to develop tools to retrieve comprehensive information on phytoplankton in the ocean at regional scales using remotely-sensed data. In this section, the boundaries of the ecological provinces of the North-West Atlantic (Fig. 5) as defined by Sathyendranath *et al.* (1995) and Longhurst (1998) are refined using satellite-derived chlorophyll-a concentrations and sea-surface temperatures. An algorithm to discriminate diatom-dominated phytoplankton populations from other populations is also applied and the results are interpreted in the context of the dynamic boundaries of the ecological provinces. Spring and Autumn 2003 are the two seasons selected to illustrate the relationship between the boundaries of the ecological provinces and the distribution of phytoplankton functional groups.

Daily images of sea-surface temperature and chlorophyll-a concentration were acquired between April 24th and May 15th, 2003 (Spring) and between

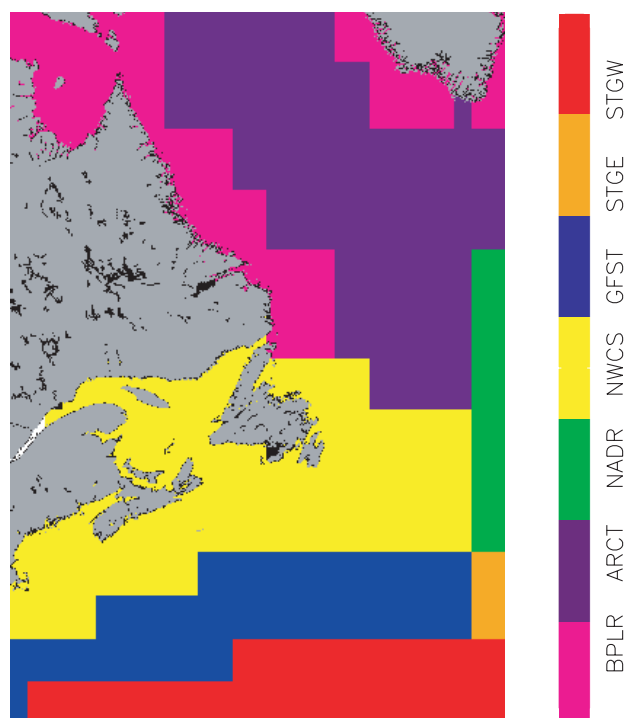


Fig. 5. – The ecological provinces in the North-West Atlantic as defined by Sathyendranath *et al.* (1995).

October 13th and October 28th, 2003 (Autumn) using AVHRR and SeaWiFS data, respectively. These dates correspond to the dates of scientific cruises carried out as part of the Canadian SOLAS (Surface-Ocean Lower Atmosphere) programme in which *in situ* data were collected to validate the products (not presented in this paper). Discrimination of diatoms from other populations (hereafter referred to as “mixed population”) was also performed on the ocean-colour data. The algorithm used to achieve this (Sathyendranath *et al.*, 2004) is based on the absorptive properties of diatoms, which differ from those of other phytoplankton populations (typically smaller cells), and a theoretical reflectance model (Sathyendranath and Platt, 1997), which relates water-leaving reflectances to chlorophyll concentration.

The procedure to identify the phytoplankton for a given pixel in an image includes four steps: i) two chlorophyll-a concentrations were computed with algorithms for diatom-dominated populations that used two different ratios of water-leaving reflectances (the two wavelength pairs used were 490:670 and 510:555); ii) this was repeated with the algorithms for mixed populations; iii) the difference in the two chlorophyll-a values obtained for the diatom-dominated case was divided by their mean value, to obtain the normalised difference in chloro-

phyll concentrations, and the computation was repeated for the non-diatom case; iv) the pixel was classified as diatom-dominated or otherwise, depending on which algorithm yielded the smaller normalised difference. The assumption here is that the differences in estimated chlorophyll obtained using different pairs of wavebands will be less when the diatom model is applied to a diatom-dominated location or when a mixed-population model is applied to a location with mixed populations, rather than when there is a mismatch between assumption and reality. This is a binary approach where pixels are classified either as dominated by diatoms (assigned a value of 100%) or dominated by a mixed population (assigned a value of 0%). This procedure was repeated for every pixel and for all images available during the time of the study. All the processed images for Spring and Autumn were used to generate seasonal composite images which show the number of times a pixel was classified as diatoms divided by the total number of images with valid data in that pixel location (that is to say, images with cloudy conditions or negative chlorophyll concentrations at that pixel location were not included when computing this ratio). These composite images may be interpreted as showing on a pixel-by-pixel basis the probability that the phytoplankton was diatom dominated, for the time intervals for which the images were created.

Composite images of the North-West Atlantic showing the probability of the presence of diatoms in Spring and Autumn of 2003, are shown in Figure 6. Mapping the distribution of diatoms over large scales reveals features that cannot be observed using *in situ* measurements collected from scientific ships. The left-hand-side image shows an intense bloom of diatoms during the Spring in the southern region of the Scotian Shelf. At high latitudes, diatoms are also present, probably the result of ice melt, and subsequent increase in nutrient supply. In the Autumn image, diatoms are dominant on Georges Bank, which is consistent with the field observations of Hoepffner and Sathyendranath (1992, 1993). The diatom blooms that started in the spring season have shifted further north. The presence of diatoms off the mouth of the Saint Lawrence River may be the result of high nutrients caused by the river discharge (assuming that the algorithm is not in error in these potentially Case-2 waters).

Partitioning the ocean into biogeochemical provinces is a useful concept to assign biological properties based on physical forcing. To date, such

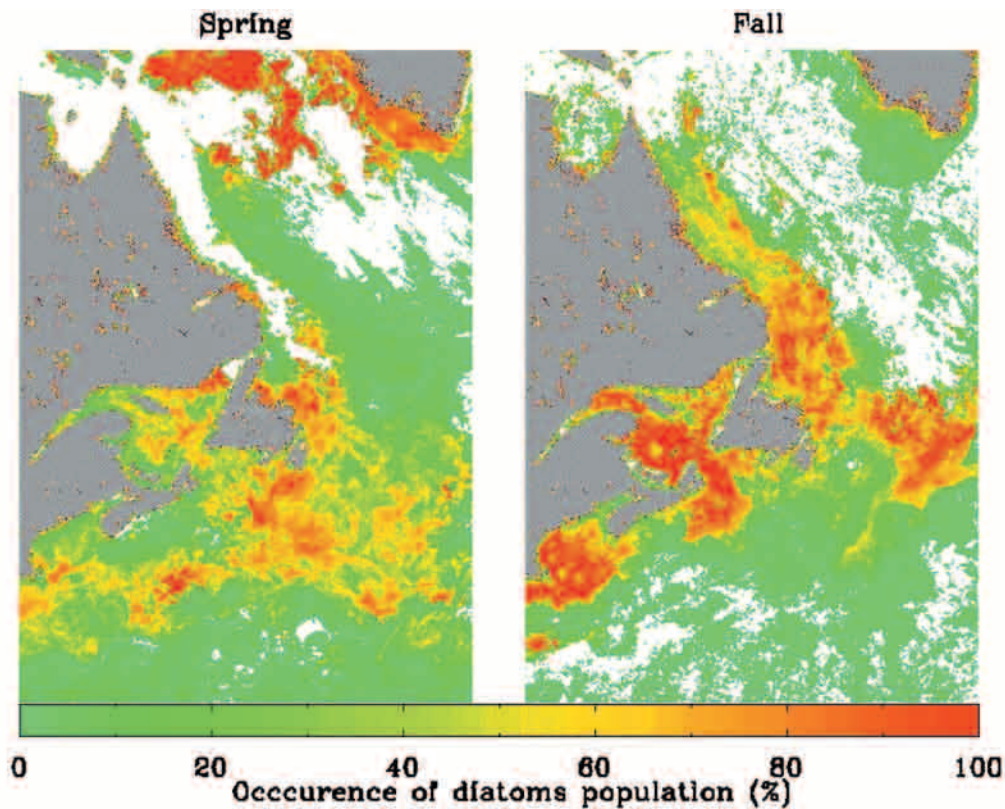


Fig. 6. – Composite images of diatoms population identification for the Spring and Fall 2003 in the North-West Atlantic.

partitions have been used mainly for pedagogical applications rather than for operational oceanography. We have developed a simple operational method to divide the North-West Atlantic Ocean into provinces using sea-surface temperatures and chlorophyll-a concentrations retrieved by satellite as primary indicators, and location and bathymetry as secondary indicators. According to the conventional, static partition of Longhurst *et al.* (1995), Sathyendranath *et al.* (1995) and Longhurst (1998) the study area was first divided into 7 provinces:

- Three provinces were characterized as warm oligotrophic regions (Eastern and Western part of the Subtropical gyre, STGW and STGE respectively, and the Gulf Stream, GFST);

- Two provinces were characterized by colder waters (Polar Boreal current, BPLR, and Arctic waters, ARCT);

- One province represented the continental shelf (NWCS); and

- The North Atlantic Drift (NADR) represented the water mass that results from the mixture of Arctic and oligotrophic waters.

For each of the provinces as defined by the boundaries in Figure 5, the frequency distributions of sea-surface temperature and chlorophyll concen-

tration were plotted (Fig. 7 and 8). Multiple peaks in the sea-surface temperature histograms indicate that different water masses are present within the same putative province. Moreover, the same peaks in sea-surface temperature distribution may be found in different provinces: for instance a peak of temperature occurs at 21°C in the STGW and GFST provinces, or at 3.5°C in the BPLR and ARCT waters. Similar features are also observed in the chlorophyll histograms. These observations indicate that the static partition is less than perfect, and that the provincial boundaries should be readjusted dynamically.

Therefore, the boundaries of provinces were reorganized using an interactive procedure based on visual analysis of the frequency distributions of the sea-surface temperature and chlorophyll concentration in each province. Thus, the following four criteria were applied:

- Only a single sea-surface temperature peak should appear in each provinces, as far as possible;

- Chlorophyll concentration was used as an indicator of water masses when the partitioning could not be based on sea-surface temperature alone (for instance, North Atlantic Drift had similar sea surface temperatures as continental shelf);

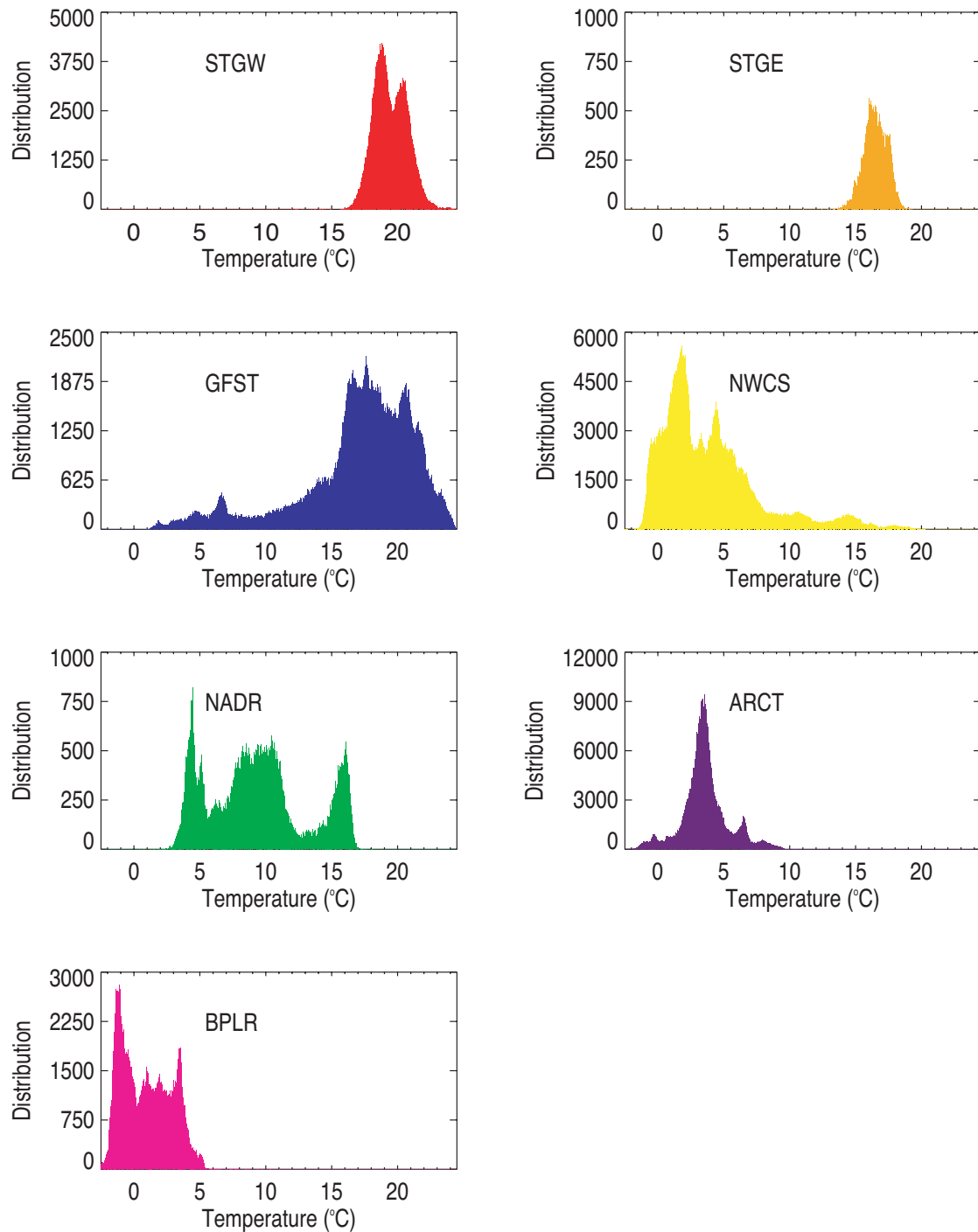


Fig. 7. – Frequency distribution of sea surface temperatures for the spring season extracted from the composite image for the provinces defined by Sathyendranath *et al.* (1995).

- Bathymetry helped to separate provinces along a front where the gradients of chlorophyll-a concentration and sea-surface temperatures on both sides of the front did not allow identification of the provinces (e.g., Boreal Polar waters and Arctic waters) and;

Location was also used in a broad sense. That is to say, we made an *a priori* decision, based on

knowledge of the regional oceanography, that the provincial boundaries will be found in the neighbourhood of the static boundaries as defined by Longhurst (1998). For example, if similar temperatures are found in disparate locations, they are treated as indicators of distinct provinces: for example, continental shelf waters and the waters off Greenland may have similar temperatures, but

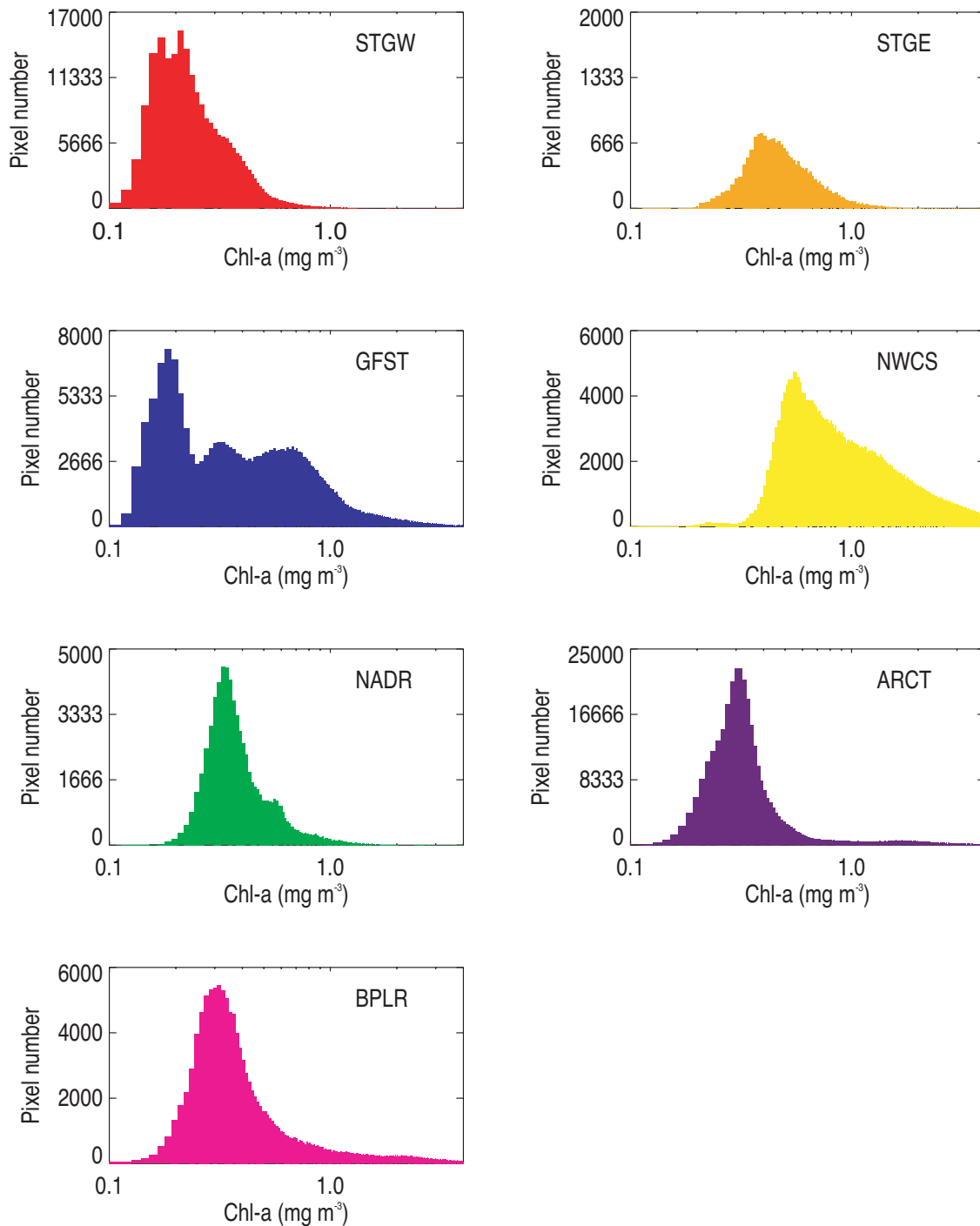


Fig. 8. – Frequency distribution of chlorophyll concentrations for the spring season extracted from the composite image for the provinces defined by Sathyendranath *et al.* (1995).

do not belong to the same province. However, the method allows a “peppering” effect in the neighbourhood of boundaries, representing incursions of neighbouring waters across boundaries.

To the provinces defined in Sathyendranath *et al.* (1995) (albeit with their boundaries reassigned dynamically), a new province was added, which we named “Slope Waters”, taking in waters lying

between the NWCS province and the warm oligotrophic waters. These waters have the same range of chlorophyll concentration as the oligotrophic waters, but have the same range of sea-surface temperatures as the continental shelf waters. Figure 9 shows the log-normal frequency distributions of sea-surface temperatures and chlorophyll-a concentrations after pixels were classified into

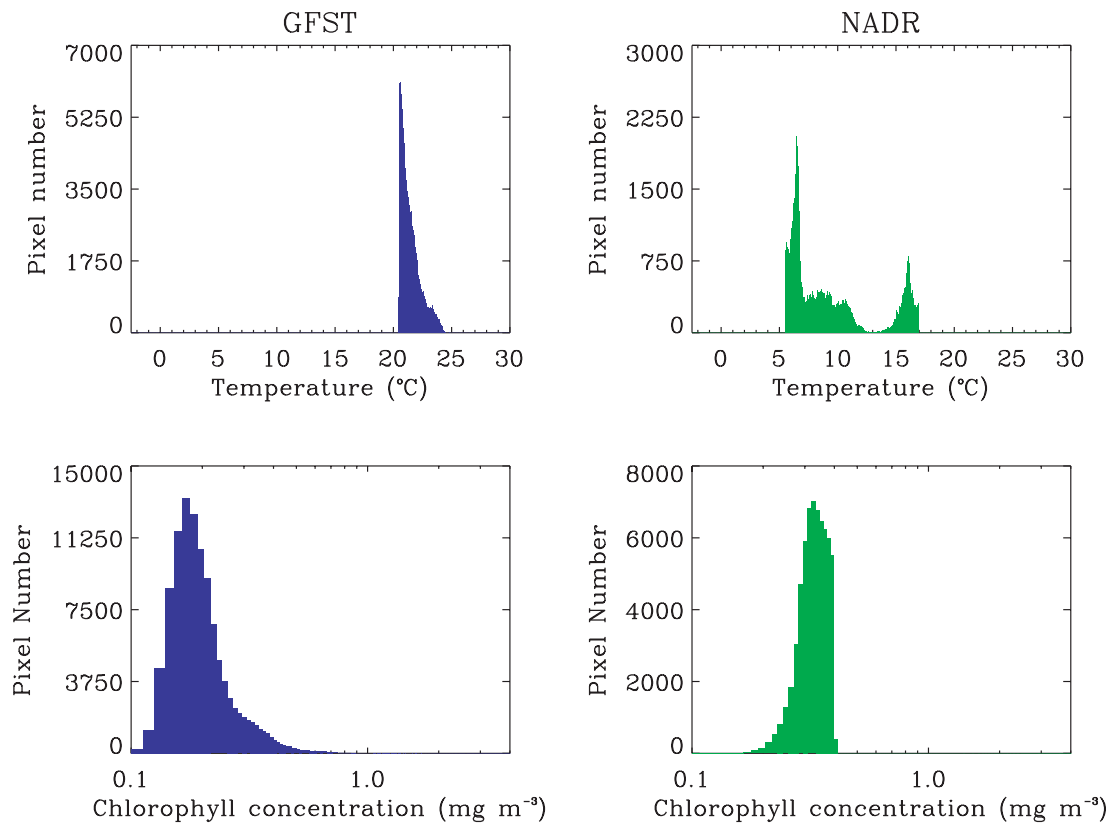


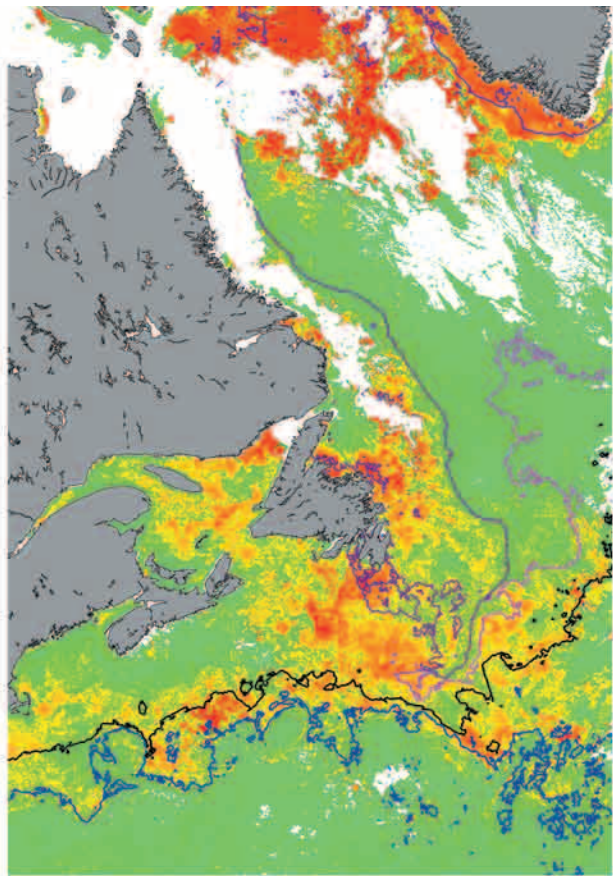
Fig. 9. – Frequency distribution of sea surface temperatures and chlorophyll concentrations for the spring season extracted from the composite image after application of criteria to determine the provinces dynamic boundaries.

ecological provinces using the steps outlined above for two of the provinces.

The same method of assigning provincial boundaries based on satellite observations was applied to images obtained in Autumn. The sea-surface temperature criteria were modified to account for the increase in sea-surface temperatures as a result of summer heating over the study area. Biomass concentration criteria were also modified to account for differences in the intensity and distribution of blooms. Comparison of provincial boundaries in Spring and Autumn shows a movement of the oligotrophic warm waters (Gulf Stream and sub-tropical gyre) towards the north (Figs. 10, 11). It is also noteworthy that the Boreal Polar Region extends south during the Autumn season into the slope waters, following the 1000-to-2000 m isobath, even though bathymetry was not used as a criterion to define this boundary.

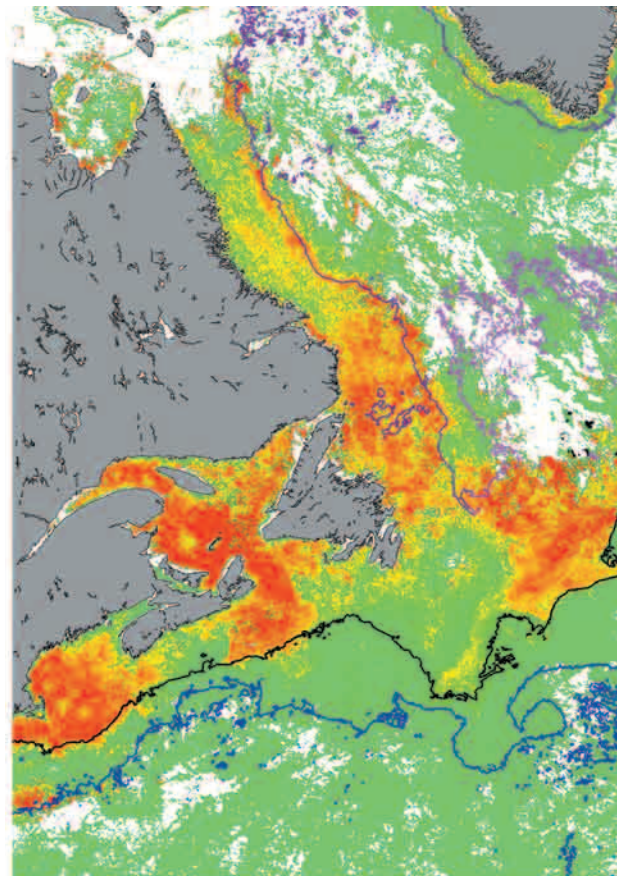
The boundaries of biogeochemical provinces and the distribution of diatoms show similar features (Figs. 10, 11). This is not unexpected, since chlorophyll biomass was used to define the provinces and diatom blooms are known to appear

at higher chlorophyll concentrations (see Fig. 3). Similarly, temperature distribution was used to estimate the boundaries of provinces, and temperature is also related to community structure, as shown earlier (Fig. 2). In the southern part of the study area, during Spring, the diatom blooms occur in the slope waters and on the North-West Continental Shelf, and a clear front is observed with the southern oligotrophic waters where no diatoms were identified. Diatoms are also identified in the Boreal Polar Region in the Spring and the Autumn between 50 and 55°N at the border with the Arctic waters. In Autumn, an intense bloom of diatoms occurred in the eastern part of the slope waters and spread into the North Atlantic Drift waters. The relationship between water masses and groups of phytoplankton is illustrated here for the first time using remotely-sensed data. It demonstrates the complementarity of *in situ* measurements, which showed strong relations between physical properties, phytoplankton groups and their physiology, and remotely-sensed ocean-colour data, justifying extrapolation of the *in situ* model to wide areas using suitable algorithms.



0 20 40 60 80 100
 Occurrence of diatoms population (%)
 — Boreal Polar waters boundary
 — Oligotrophic waters boundary
 — Slope waters boundary
 — Arctic waters boundary

Fig. 10. – Composite image of identification of diatoms during spring. Solid lines correspond to the province boundaries.



0 20 40 60 80 100
 Occurrence of diatoms population (%)
 — Boreal Polar waters boundary
 — Oligotrophic waters boundary
 — Slope waters boundary
 — Arctic waters boundary

Fig. 11. – Composite image of identification of diatoms during autumn. Solid lines correspond to the province boundaries.

TEMPORAL DEVELOPMENT OF A DIATOM BLOOM FOLLOWING A STORM

In the ocean, the passage of a hurricane leads to enhanced entrainment of cold, nutrient-rich water into the mixed layer. The entrainment process promotes increased primary production and therefore higher phytoplankton biomass (chlorophyll-a). The arrival of remote sensing has improved our capacity to measure synoptic fields of oceanographic processes to assess these powerful transient events in different regions of the world (Fuentes-Yaco *et al.*, 1997; Nayak *et al.*, 2001; Subrahmanyam *et al.*,

2002; Zedler *et al.*, 2002; Lin *et al.*, 2003; McKinnon *et al.*, 2003; Vinayachandran and Mathew, 2003; Babin *et al.*, 2004; Vinayachandran *et al.*, 2004). Eastern Canada can experience several hurricanes each year. In 2003, the hurricane season in the Atlantic Ocean was very active, with 14 named storms. Typically, the storms progress northwards along the eastern seaboard of the United States, and then turn to the east affecting the Scotian Shelf and/or the Newfoundland Shelf. Here we examine the response of the fields of chlorophyll and temperature, and the community structure of phytoplankton, to the passage of Hurricane Kate.

This hurricane crossed the Grand Banks of Newfoundland, an area with rich fisheries resources.

According to the National Hurricane Center of the National Weather Service (NOAA), Hurricane Kate was born as a tropical wave that crossed the coast of Western Africa on September 21st. By October 4th the hurricane reached its strongest wind intensity (185 km h⁻¹), when it was east-southeast of Bermuda. On October 5th and 6th, the cyclone turned northward then accelerated to north-east over cooler waters. As reported by the Meteorological Service of Canada - Atlantic, Hurricane Kate was in the Response Zone of the Canadian Hurricane Centre between the 7th and 8th of October (Fig. 12), entering the region as a Category-1 Hurricane (110 to 120 km h⁻¹), and was at tropical-storm strength as it moved through the South-Eastern and Northern Grand Banks of Newfoundland. The system completed its extra-tropical transition by October 8th.

The response of the fields of chlorophyll and temperature to the passage of Hurricane Kate in the North-West Atlantic (39 to 62.5°N and 42 to 71°W) was studied using satellite images of ocean colour (SeaWiFS) and sea-surface temperature (NOAA/AVHRR). Daily images of chlorophyll-a, an index of phytoplankton biomass, were created following a method that accounts for changes in the absorptive properties of different phytoplankton populations (Sathyendranath *et al.*, 2004). Sea-surface temperatures (SST) were calculated as established by McClain *et al.* (1985). Composite images were produced with all available images from 12 days before (September 25th to October 6th, 2003) to 14 days after (October 7th to 20th, 2003) the storm passage. They were made on a spatial scale of approximately 1.5 km to preserve the detailed spatial structure, and used to extract data in the Canadian region across a band of 700 km following the storm track: 350 km on the left side and 350 km on the right side (Fig. 12).

Changes in sea-surface temperature and chlorophyll-a concentration

The passage of a storm, with strong associated winds, can generate upwelling of cold water from the deep layers along its trajectory. This mechanism brings nutrients to the surface, supporting the development of remarkable phytoplankton blooms. Figure 12 (a and b) shows sea-surface temperature, which may be considered as a proxy for nutrient entrainment to the surface layers (Sathyendranath

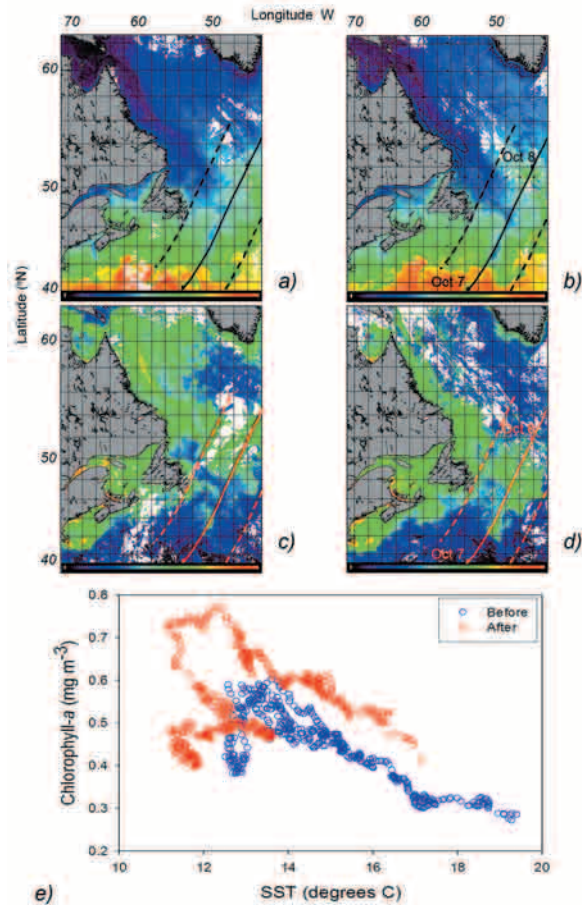


Fig. 12. – Composites of sea surface temperature: a) 12 days before the passage of Hurricane Kate, from September 25th to October 6th, and b) 14 days after the passage of the storm, October 7th to 20th, 2003. Composites of chlorophyll-a concentration: c) 12 days before, and d) 14 days after the hurricane passage. The storm track and a band of 700 km (350 km on both sides) are also indicated. e) Scatter plot of sea surface temperature against chlorophyll-a. The data are extracted from the composite images under the 700 km area, and averaged across the storm track.

et al., 1991). The left side (a) corresponds to the period before the storm passage and the right side (b) to the period after the storm passage. Figure 12 (c and d), shows the fields of chlorophyll-a before (c) and after (d) the storm passage. In the composites after the storm passage (right side maps), strong gradients of both sea-surface temperature and chlorophyll-a are clearly visible in the vicinity of the Grand Banks of Newfoundland. Additional analyses based on data extracted from the composite images in a band of 700 km, and averaged across the storm track (this approach to extraction and averaging was also used for the other figures shown here from this analysis), confirm that cooler waters were associated with stronger pigment concentrations, and this relationship appeared to be more robust after, than before, the storm passage (Fig. 12e).

A detailed analysis of changes along and across the storm track is shown in the subsequent figures. Figure 13a and 13b show concurrent changes in sea-surface temperature and chlorophyll-a under the area along the storm track. Figure 13a shows the difference (after - before) in sea-surface temperature, whereas Figure 13b shows relative change in chlorophyll-a (as ratio of pigment after to pigment before, passage of storm), both computed using the composite images of before and after the hurricane passage. The right side of the storm path shows complex features in changes of temperature with differences up to 7°C (Fig. 13a). These structures are coherent with changes in chlorophyll-a, from three

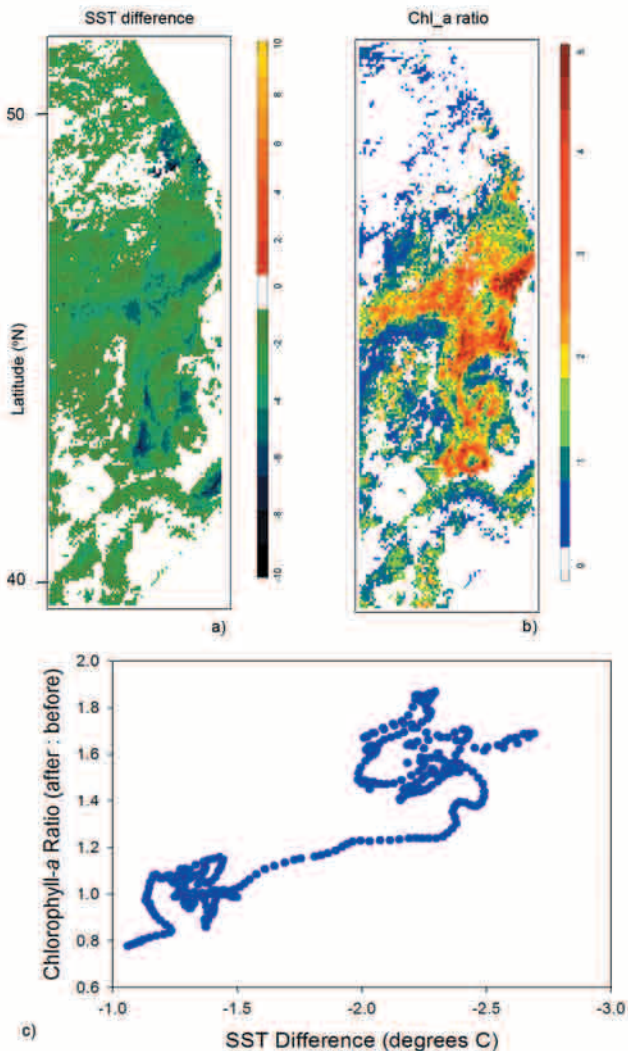


Fig. 13. – Changes in sea surface temperature and chlorophyll-a: a) Difference (after-before) in SST. Green and blue colours show decreased temperatures. b) Ratio (after : before) of chlorophyll-a. Values above 1.0 indicate areas where the phytoplankton biomass increased. c) Scatter plot of concurrent changes in SST (difference) and Chl-a (ratio). The data are extracted from the composite images within a 700 km band (see Fig. 12), and averaged across the storm track. The low (or high) values of change are related with the left (or right) side of the storm track.

to six fold (Fig. 13b). It reveals in great detail the impact of Hurricane Kate on the pelagic ocean.

Data of the concurrent changes in sea-surface temperature and phytoplankton pigment (Fig. 13c) show an imbalance in the distribution of the differences in SST and Chl-a. Pixels with small differences appear the left side of the storm, whereas those with big differences are seen to the right side of the storm path. These results coincide with previous observations concerning the stronger effect of the storms passage on the right side than on the left side of storm tracks (Iverson, 1997). It is also important to note that the right side of the hurricane crossed the South-Eastern slope of the Grand Banks of Newfoundland, the area with the greatest measured variations. The stronger upwelling of cold water (with high nutrient concentrations) apparently triggered a strong biological response.

Impact of physical forcing on ecosystem structure

Margalef (1978) proposed that, in the marine environment, species succession is heavily influenced by two physical processes: advection and turbulence. He also postulated that in addition to light energy, the kinetic energy provided by wind and waves also drives the production in aquatic ecosystems by modifying nutrient supply and temperature. Furthermore, Margalef (1978) also proposed a systematization of the functional morphology of phytoplankton on the basis of two basic environmental factors: supply of nutrients and intensity of turbulence. In this context, it is known that the taxonomic composition of phytoplankton communities is regulated by physical processes, and that temperature is a suitable proxy for nutrient (new nitrogen) supply (Bouman *et al.*, 2003). Estrada and Berdalet (1997) underline that diatoms, non-motile organisms with fast potential growth rates, prosper in relatively turbulent and nutrient-rich waters. These characteristics make diatoms ideal organisms to illustrate the response of community structure to the passage of a major storm, and to test whether turbulent and nutrient-rich waters prevailing after a hurricane passage can be suitable for their growth.

Here, the use of an algorithm that allows distinction between diatoms from other phytoplankton populations (Sathyendranath *et al.*, 2004) provides additional information to assess phytoplankton blooms. Figure 14 shows composite images of the probability of finding diatoms: the left image (a)

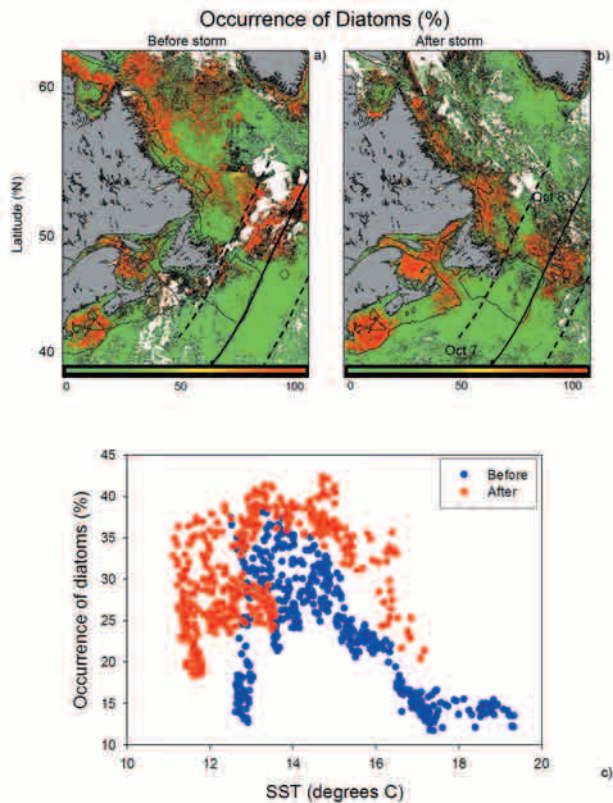


Fig. 14. – Composites of probability to find diatom dominant populations: a) 12 days before the storm passage, and b) 14 days after the hurricane passage. c) Scatter plot of SST against probability to find diatoms. The data are extracted from the composite images under the 700 km area, and averaged across the storm track.

corresponds to the period before the passage of Hurricane Kate and the right composite (b) corresponds to the period after the passage of the storm. Before the storm passage, diatoms seemed to be dominant in the northern area (50 to 55°N) of the path; however, after the storm passage, the northern bloom seemed to disappear and a new diatom bloom developed between 45 and 50°N. The strongest probabilities to find diatoms were on the right side of the storm track, corresponding to the slope of the Grand Banks of Newfoundland. Simultaneous data of sea-surface temperature and the probability of finding diatoms are shown in Figure 14c. It is interesting to see how the probabilities to find diatoms increased after the storm passage, as the temperature decreased. This pattern is similar to the relationship found between phytoplankton biomass and sea-surface temperature (Fig. 12).

The change in probability of finding diatoms can be estimated by computing the differences in probabilities before and after the storm passage, using the composite images (Fig. 15a). Figure 15b shows the differences of sea-surface temperature against the

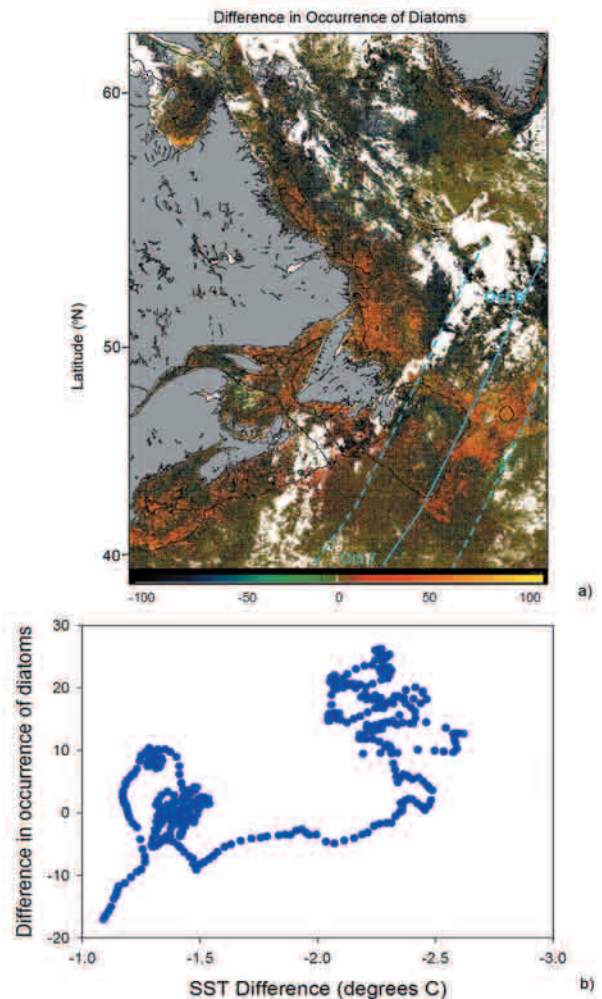


Fig. 15. – Differences (composite after - composite before) in the probability to find diatom-dominated populations (a). Red to yellow (positive values) colour denote increased probabilities. Green to blue colours (negative values) show decreased probabilities. Scatter plot of differences of SST against differences of probability to find diatoms dominance (b). The data are extracted from the composite images under the 700 km area, and averaged across the storm track. The low (or high) values of change are related with the left (or right) side of the storm track.

differences in the probability of finding diatoms. The distribution shows an asymmetry, with low values on the left and high values on the right side of the storm path. It is possible that the extreme mixing created by the strong winds related to the hurricane could restrict the growth of diatoms already present before the storm. After the passage of the hurricane, a new stability gradient was apparently created and triggered a new phytoplankton succession cycle, led by diatoms.

Using a temporal series of two-day composite images, we also examined the development of diatom blooms over time, in response to the presumed entrainment of nitrate into the surface layer

by wind mixing (Fig. 16). A two-day period allowed reduction in the proportion of cloud cover masking the images, but provided sufficient temporal resolution to observe the biological response to the storm. The geographic distributions of the ecological provinces obtained using the method described in the previous section are also shown for before, and after, the passage of the storm (Fig. 16). Note that the maps of the provinces for both before and after the storm are derived from 12-day composite images.

The presence of diatoms is apparent before the passage of the storm in the northern part of the images corresponding to the Arctic Province. In the southern region, which is designated predominantly as the Slope Province, diatoms are generally absent, except for a few very small patches. The map of the provinces before the storms shows an incursion of Boreal Polar waters into the slope waters that tends to follow the steep slope of the Scotian Shelf. After the passage of the storm (S+1 to S+11), diatoms tend to predominate in the center of the image, between 42 and 44°N and increase in relative abundance the following four days. This event corresponds to an intrusion of Boreal Polar waters into this area, suggesting that the mixing of waters by the storm deepened the mixed layer, leading to a supply of nutrients to the surface ocean. This temporal analysis emphasizes the impact of storms on marine ecosystems. The passage of the storm in a nutrient-depleted environment (south part of the image) resulted

not only in an increase in phytoplankton biomass, but also a change in the community structure. The northern part of the area, where diatoms were already present, were less impacted, as ocean colour data showed a decrease in chlorophyll concentration (probably due to a redistribution of existing biomass over a deeper mixed layer).

CONCLUDING REMARKS

The broad lines of the majestic partition of the oceans by Longhurst (1998) follow from the premise that the spatial features of phytoplankton distributions are under the control of physical forcing, and that the temporal changes in these distributions reflect changes in the relevant physical forcing. We have shown that this premise is justified by the available observations on the physiological ecology of phytoplankton in relation to the physical properties of the environment. Moreover, we have shown for the first time that the ocean partition of Longhurst can be implemented in the operational mode using remotely-sensed data as input. The resulting partition corresponds broadly with the Longhurst one, but differs in detail and in that the boundaries can be adjusted in real time to reflect changes in forcing. These boundaries are consistent with what is known about the community structure of the phytoplankton. Finally, using remotely-sensed data on ocean colour, we have documented

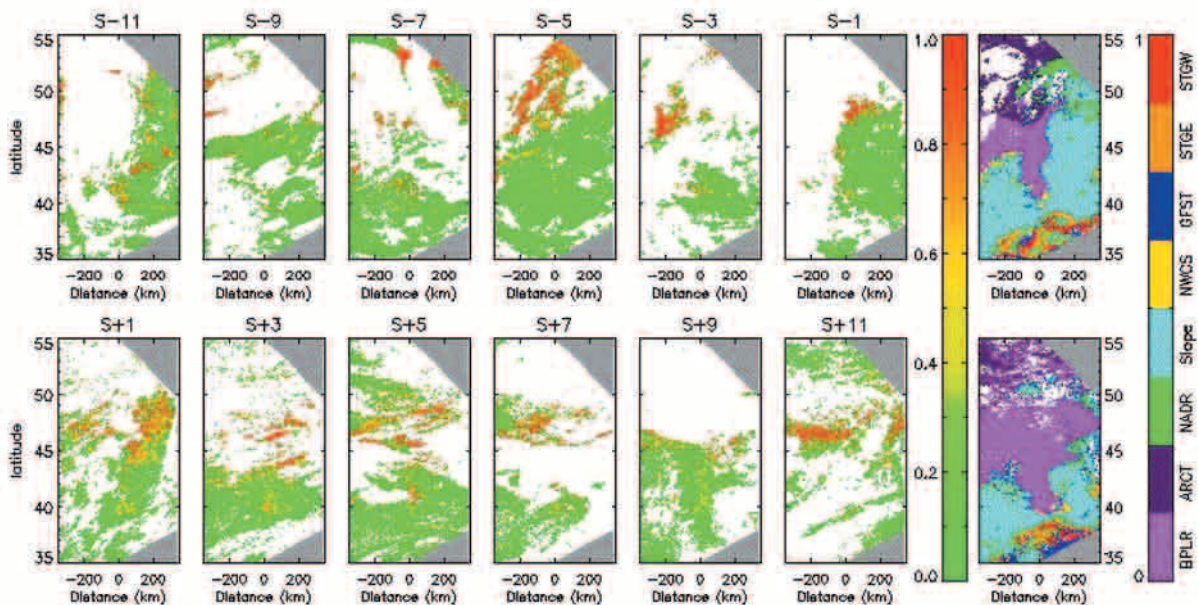


Fig. 16. – Temporal series of two-day composite images of the probability of occurrence of a diatom-dominated population along the storm track 12 days before (top) and 12 days after (bottom) the passage of the hurricane. Data were averaged across the storm track within a 700 km band (see Fig. 12). Plots on the right-hand side indicates the biogeochemical provinces before and after the storm.

the response of the phytoplankton biomass, and of community structure, to the passage of a hurricane across the eastern seaboard of Canada. These observations reinforce the views of Margalef (1978) and of Longhurst (1998) concerning the influence of physical forcing on phytoplankton distributions (*sensu largo*) and enhance the value of remotely-sensed data of ocean colour as a means to illustrate and characterise this relationship.

ACKNOWLEDGEMENTS

This paper is part of the Canadian SOLAS programme. This work is also sponsored by the Canadian Space Agency.

REFERENCES

- Babin S.M., J.A. Carton, T.D. Dickey and J.D. Wiggert. – 2004. Satellite evidence of hurricane-induced phytoplankton blooms in an oceanic desert. *J. Geophys. Res.*, 109: C03043, doi:10.1029/2003JC001938.
- Behrenfeld M.J., E. Marañon, D.A. Siegel, and S.B. Hooker. – 2002. Photoacclimation and nutrient-based model of light-saturated photosynthesis for quantifying oceanic primary production. *Mar. Ecol. Prog. Ser.* 228: 103-117.
- Bouman H. A., T. Platt, S. Sathyendranath, W. K. W. Li, V. Stuart, C. Fuentes-Yaco, H. Maass, E. P. W. Horne, O. Ulloa, V. Lutz and M. Kyewalyanga. – 2003. Temperature as indicator of optical properties and community structure of marine phytoplankton: implications for remote sensing. *Mar. Ecol. Prog. Ser.*, 258: 19-30.
- Bouman, H.A., T. Platt, S. Sathyendranath and V. Stuart. – In press. Dependence of light-saturated photosynthesis on temperature and community structure. *Deep-Sea Res.*
- Carder, K.L., F.R. Chen, Z.P. Lee, S.K. Hawes and D. Kamrowski. – 1999. Semianalytic Moderate-Resolution Imaging Spectrometer algorithms for chlorophyll a and absorption with bio-optical domains based on nitrate-depletion temperatures. *J. Geophys. Res.*, 104: 5403-5421.
- Chisholm, S.W. – 1992. Phytoplankton size. In: P.G. Falkowski and A.D. Woodhead (eds.), *Primary Productivity and Biogeochemical Cycles in the Sea*. pp. 213-237. Plenum Press, New York.
- Ciotti, A.M., J.J. Cullen and M.R. Lewis. – 1999. A semi-analytical model of the influence of phytoplankton community structure on the relationship between light attenuation and ocean colour. *J. Geophys. Res.*, 104: 1559-1578.
- Ciotti, A.M., M.R. Lewis and J.J. Cullen. – 2002. Assessment of the relationships between dominant cell size in natural phytoplankton communities and the spectral shape of the absorption coefficient. *Limnol. Oceanogr.*, 47: 404-417.
- Claustre, H.M. – 1994. The trophic status of various oceanic provinces as revealed by phytoplankton pigment signatures. *Limnol. Oceanogr.*, 39: 1206-1210.
- Côté, B. and T. Platt – 1983. Day-to-day variations in the spring-summer photosynthetic parameters of coastal marine phytoplankton. *Limnol. Oceanogr.*, 28: 320-344.
- Côté, B. and T. Platt. – 1984. Utility of the light-saturation curve as an operational model for quantifying the effects of environmental conditions on phytoplankton photosynthesis. *Mar. Ecol. Prog. Ser.*, 18: 57-66.
- Cullen, J.J., P.J.S. Franks, D.M. Karl and A. Longhurst. – 2002. Physical influences on marine ecosystem dynamics. In: A.R. Robinson, J.J. McCarthy and B.J. Rothchild (eds.), *The Sea - Volume 12*. pp. 297-336. Wiley, New York.
- Duysens, L.M.N. – 1956. The flattening of the absorption spectrum of suspensions, as compared to that of solutions. *Biochim. Biophys. Acta*, 19: 1-12.
- Eppley, R.W. – 1972. Temperature and phytoplankton growth in the sea. *Fish. Bull.*, 70: 1063-1085.
- Estrada M. and E. Berdalet. – 1997. Phytoplankton in a turbulent world. *Sci. Mar.* 61: 125-140.
- Finkel, Z.V. – 2001. Light absorption and size scaling of light-limited metabolism in marine diatoms. *Limnol. Oceanogr.*, 46: 86-94.
- Fuentes-Yaco, C., A.F. Vézina, M. Gosselin, Y. Gratton, and P. Larouche. – 1997. Influence of late-summer storms on the horizontal variability of phytoplankton pigment determined by Coastal Zone Color Scanner images in the Gulf of St. Lawrence, Canada. In: S.G. Ackleson and R. Frouin (eds.), *Ocean Optics XIII*, Proc. SPIE 2963: 678-683.
- Geider, R.J. and B.A. Osborne. – 1992. *Algal Photosynthesis: The Measurement of Algal Gas Exchange*. Chapman and Hall, New York.
- Geider, R. J., T. Platt and J.A. Raven. – 1986. Size dependence of growth and photosynthesis in diatoms: A synthesis. *Mar. Ecol. Prog. Ser.*, 30: 93-104.
- Head, E.J.H. and E.P.W. Horne. – 1993. Pigment transformation and vertical flux in an area of convergence in the North Atlantic. *Deep-Sea Res. II*, 40: 329-346.
- Hoepffner N. and S. Sathyendranath. – 1992. Bio-optical characteristics of coastal waters: absorption spectra of phytoplankton and pigment distribution in the North-West Atlantic. *Limnol. Oceanogr.*, 37: 1660-1679
- Hoepffner N. and S. Sathyendranath. – 1993. Determination of the major groups of phytoplankton pigments from the absorption spectra of total particulate matter. *J. Geophys. Res.*, 982: 22789-22803.
- Iverson, R.L. – 1997. Mesoscale oceanic phytoplankton patchiness caused by hurricane effects on nutrient distribution in the Gulf of Mexico In: N.R. Andersen and B.J. Zahuranec (eds.), *Oceanic Sound Scattering Prediction*. pp. 767-778. Plenum Press, New York.
- Laws, E.A., P.G. Falkowski, W.O. Smith, H. Ducklow and J.J. McCarthy. – 2000. Temperature effects on export production in the open ocean. *Global Biogeochem. Cycles*, 14: 1231-1246.
- Lin, I., W.T. Liu, C-C. Wu, G.T.F. Wong, C. Hu, Z. Chen, W-D Liang, and K-K Liu. – 2003. New evidence for enhanced ocean primary production triggered by tropical cyclone. *Geophys. Res. Lett.*, 30: 1718, doi:10.1029/2003GL017141.
- Li, W.K.W. – 2002. Macroecological patterns of phytoplankton in the northwestern North Atlantic Ocean. *Nature*, 419: 154-157.
- Li, W.K.W. – In press. Plankton populations and communities. In: J. Witman and K. Roy (eds.), *Marine Macroecology*. University of Chicago Press.
- Longhurst, A.R. – 1998. *Ecological geography of the seas*. Academic Press, San Diego.
- Longhurst, A.R., S. Sathyendranath, T. Platt and C.M. Caverhill. – 1995. An estimate of global primary production in the ocean from satellite radiometer data. *J. Plankton Res.*, 17: 1245-1271.
- Margalef, R. – 1978. Life-forms of phytoplankton as survival alternatives in an unstable environment. *Oceanol. Acta*, 1: 493-509.
- McClain, E. P., W.G. Pichel, and C.C. Walton. – 1985. Comparative performance of AVHRR-based multichannel sea surface temperatures. *J. Geophys. Res.*, 90: 11587-11601.
- McKinnon, A. D., M.G. Meekan, J.H. Carleton, M.J. Furnas, S. Duggan and W. Skirving. – 2003. Rapid changes in shelf waters and pelagic communities on the southern Northwest Shelf, Australia, following a tropical cyclone. *Cont. Shelf Res.*, 23: 93-111.
- Nayak, S.R., R. K. Sarangi and A.S. Rajawat. – 2001. Application of IRS-P4 OCM data to study the impact of cyclone on coastal environment of Orissa. *Cur. Sci.*, 80: 1208-1213.
- Platt, T. and A.D. Jassby. – 1976. The relationship between photosynthesis and light for natural assemblages of coastal marine phytoplankton. *J. Phycol.* 12: 421-430.
- Platt, T. and S. Sathyendranath. – 1988. Oceanic primary production: estimation by remote sensing at local and regional scales. *Science*, 241: 1613-1620.
- Platt, T. and S. Sathyendranath. – 1999. Spatial structure of pelagic ecosystem processes in the global ocean. *Ecosystems*, 2: 384-394.
- Platt, T., C.L. Gallegos and W.G. Harrison. – 1980. Photoinhibition of photosynthesis in natural assemblages of marine phytoplankton. *J. Mar. res.*, 38: 687-701.

- Rodríguez, J., J.M. Blanco, F. Jiménez-Gómez, F. Echevarria, J. Gil, V. Rodríguez, J. Ruiz, B. Bautista and F. Guerrero. – 1998. Patterns in the size structure of the phytoplankton community in the deep fluorescence maximum of the Alboran Sea (south-western Mediterranean). *Deep-Sea Res.*, 45: 1577-1593.
- Rodríguez, J., J. Tintoré, J.T. Allen, J.M. Blanco, D. Gomis, A. Reul, J. Ruiz, V. Rodríguez, F. Echevarria and F. Jiménez-Gómez. – 2001. Mesoscale vertical motion and the size structure of phytoplankton in the ocean. *Nature*, 410: 360-363.
- Sathyendranath, S., A. Longhurst, C. M. Caverhill and T. Platt. – 1995. Regionally and seasonally differentiated primary production in the North Atlantic. *Deep-Sea Res.*, 42: 1773-1802.
- Sathyendranath S. and T. Platt. – 1997. Analytical model of ocean color. *Appl. Optics*, 37: 2216-2227.
- Sathyendranath, S., T. Platt, E.P.W. Horne, W.G. Harrison, O. Ulloa, R. Outerbridge and N. Hoepffner. – 1991. Estimation of new production in the ocean by compound remote sensing. *Nature*, 353: 129-133.
- Sathyendranath, S., L. Watts, E. Devred, T. Platt, C. M. Caverhill and H. Maass. – 2004. Discrimination of diatoms for other phytoplankton using ocean-colour data. *Mar. Ecol. Prog. Ser.*, 272: 59-68.
- Subrahmanyam, B., K.H. Rao, N.S. Rao, V.S.N. Maurty and R.J. Sharp. – 2002. Influence of a tropical cyclone on Chlorophyll-a concentration in the Arabian Sea. *Geophys. Res. Lett.*, 29: 2051, doi:10.1029/2002GL015892.
- Switzer, A.C., D. Kamykowski, and S. Zentara. – 2003. Mapping nitrate in the global ocean using remotely sensed sea surface temperature. *J. Geophys. Res.*, 108: 3280, doi:10.1029/2000JC000444.
- Taguchi, S. – 1976. Relationship between photosynthesis and cell size of marine diatoms. *J. Phycol.*, 12: 185-189.
- Vinayachandran P.N. and S. Mathew. – 2003. Phytoplankton bloom in the Bay of Bengal during the northeast monsoon and its intensification by cyclones. *Geophys. Res. Lett.* 30: 1572, doi:10.1029/2002GL016717.
- Vinayachandran P.N., P. Chauhan, M. Mohan and S. Nayak. – 2004. Biological response of the sea around Sri Lanka to summer monsoon. *Geophys. Res. Lett.* 31: L01302, doi:10.1029/2003GL018533.
- Yentsch, C.S. and D.A. Phinney. – 1989. A bridge between ocean optics and microbial ecology. *Limnol. Oceanogr.*, 34: 1694-1705.
- Yentsch, C.S. and J.H. Ryther. – 1957. Relative significance of net phytoplankton and nannoplankton in the waters of vineyard sound. *J. Cons. int. Explor. Mer*, 24: 231-238.
- Zedler, S.E., T.D. Dickey, S.C. Doney, J.F. Price, X. Yu and G.L. Mellor. – 2002. Analyses and simulations of the upper ocean's response to Hurricane Felix at the Bermuda Testbed Mooring site: 13-23 August 1995. *J. Geophys. Res.*, 107: 3232, doi:10.1029/2001JC000969.

